JOURNAL OF CATALYSIS 138, 1–11 (1992)

Cyclopropane Isomerization over Eu^{3+}NaX Zeolites

MARK W. SIMON,* ANGELOS M. EFSTATHIOU,†,[1] C. O. BENNETT,†,‡ AND STEVEN L. SUIB*,†,‡,[2]

*U-60, Department of Chemistry; †Department of Chemical Engineering; and ‡Institute of Materials Science; University of Connecticut, Storrs, Connecticut 06269-3060

Received January 27, 1992; revised May 6, 1992

Cyclopropane isomerization to propylene over various Eu^{3+} loadings in NaX zeolite have been studied by measurements of steady-state and transient kinetics and by Fourier transform infrared spectroscopy. As Eu^{3+} loading increases, the rate of deactivation increases, the conversion increases, apparent activation energies are lowered, and Brønsted acid site strength and amounts increase. Apparent activation energies of 13–15 kcal/mol for propylene formation have been observed for these systems, consistent with literature reports for other metal supported heterogeneous catalyst systems. Deactivation studies have shown that activity can be restored by heating in He at 380°C between various temperature runs, and that gases desorbed during regeneration are predominantly propylene. Poisoning studies of Brønsted sites with Na vapor lead to deactivation of these catalysts. A reaction mechanism scheme based on π allyl intermediates in the supercages of Eu^{3+}NaX has been proposed to account for the activity, selectivity, and stability of these catalysts.

I. INTRODUCTION

We have recently reported (*1*) that cyclopropane isomerizes to propylene over Eu^{3+} NaX zeolite during sorption and desorption of cyclopropane in various diluent gases. Reports of oligomerization of cyclopropane, substituted cyclopropanes, and similar derivatives over various zeolites by other researchers (*2–4*) have suggested that C_6 oligomers can be produced. The mechanism of formation of isobutane from c-C_3H_6 over zeolites has also been a subject of debate (*5, 6*).

The purpose of this study was to investigate the effect of europium ion content in Eu^{3+}NaX zeolites on selectivity, conversion, types and amounts of acid sites, and deactivation in c-C_3H_6 isomerization. Europium (III) ions were chosen because the structure, oxidation state, and composition of such materials have been thoroughly studied by single-crystal X-ray diffraction (*7*), extended X-ray absorption fine structure (*8*), Mössbauer spectroscopy (*9*), electron paramagnetic resonance (*10*), luminescence (*8*), and luminescence lifetime measurements (*8*).

In this study, steady state kinetics have been used to obtain apparent activation energies for propylene formation as a function of Eu^{3+} loading and to investigate deactivation and regeneration of these systems. Transient kinetics have been used to compare initial rates of sorption as a function of loading and to study the numbers and amounts of surface intermediates and coke deposits during desorption. Fourier transform infrared studies with chemisorbed pyridine have been done to study the relative number of Brønsted and Lewis acid sites as a function of Eu^{3+} loading.

II. EXPERIMENTAL SECTION

A. Ion-Exchange of Zeolites

Three different loadings of Eu^{3+} in NaX zeolite were prepared via ion-exchange.

[1] Present Address: Institute of Chemical Engineering and High Temperature Chemical Processes, University of Patras, GR-26110, Patras, Greece.

[2] To whom correspondence should be addressed.

0021-9517/92 $5.00

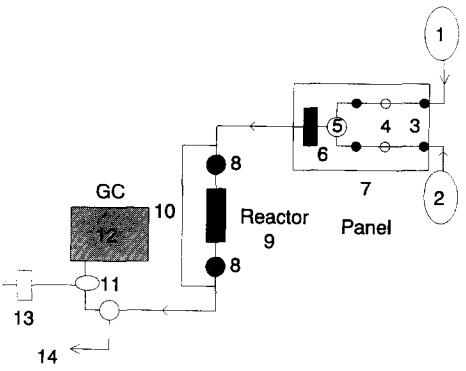

FIG. 1. Reactor system for steady-state experiments. Parts are: (1) c-C_3H_6/He mixture, (2) He, (3) 2 way, valve, (4) metering valve, (5) 3 way valve, (6) rotameter, (7) gas panel, (8) quick connect fittings, (9) reactor and furnace, (10) bypass, (11) gas sampling valve, (12) GC, (13) bubbler, and (14) vent.

About 100 ml of aqueous solutions of 0.10 *M*, 0.05 *M*, and 0.01 *M* $Eu(NO_3)_3 \cdot 6H_2O$ obtained from Alfa Ventron, Danvers, MA were used to exchange 1 g of 60-mesh NaX zeolite (Linde, from Alfa Ventron). Ion-exchanges were done at room temperature in stirred round bottom flasks overnight for 18 h followed by three washings of 5 ml of distilled deionized water. Samples were then filtered and dried in an oven at 90°C for 3 h.

B. Steady-State Catalysis

EuNaX zeolite catalyst (0.375 g) was loaded into a stainless steel reactor having a length of 12″ and an inner diameter of about 5 mm. Samples were supported by a fine stainless steel screen (100 mesh) and glass wool. Samples were dehydrated in the reactor by heating at 50° intervals for 1 h from 50 to 350°C and finally at 380°C in He with a flow rate of 30 ml/min. Final treatment temperature was held for 12 h.

A diagram of the reactor system showing the gas feed system, reactor, gas sampling valve, gas chromotograph detector, flow meters and bubblers is shown in Fig. 1. Heating tape was used on all Cu tubing lines from the reactor to the gas chromatograph (GC) to prevent sorption of products on Cu. Temperature was monitored with a digital thermometer. A vacuum pump was used to test for leaks by evacuating the line before reaction.

A thermal conductivity detector was used on a 5880 A Hewlett Packard gas chromatograph with two Poropack Q and T dual columns. An oven temperature of 120°C, an injector temperature of 175°C, and a detector temperature of 300°C were used. Helium gas was used as a carrier gas and samples were analyzed by use of an air-actuated automatic gas sampling valve having a sample loop size of 0.25 cc. A 2,000-ppm mixture of C_3H_6 was used to calibrate the signal of the TCD times before each analysis and to ensure that responses were in the linear operating range of the thermal conductivity detector.

A 9.09% cyclopropane in He feed was used for all experiments. The c-C_3H_6 was CP grade (Matheson Co.) and He was zero grade (Zero All-Gas Co.). Initial temperature of reaction was 100°C followed by studies at 120, 135, 150, and 165°C. A series of experiments was also done by keeping the temperature at 135°C and varying the partial pressure of cyclopropane from 3.8 (0.5 mol%) to 30 (3.9%) to 69 (9.1%) and finally 197 (25.9%) Torr. Regeneration of the catalyst at 380°C for 4 h under He (20 cc/min) was done after each analysis or each temperature studied. Data were collected every 10 min by using automatic programming routines. Initial conversions were between 10–12%.

Data were analyzed for the four steady-state experiments by using the material balance:

$$\text{IN} - \text{OUT} + \text{Rate} = 0 \qquad (1)$$

$$(\text{Rate}) = \text{OUT} - \text{IN}. \qquad (2)$$

or

For propylene,

$$\text{Rate} = (PQ_o/RT_o)p_{C_3H_6}/W, \qquad (3)$$

where P is total pressure (1 atm), Q_o is flow

rate in ml/sec (ambient), R is the ideal gas constant (82.057 cc-atm/mol · K), W is the weight of the catalyst, and $p_{C_3H_6}$ is the partial pressure of C_3H_6 leaving the reactor. Temperature (T_o) is in K. Rate' has units of mol C_3H_6/sec.

In addition, apparent activation energies (E_a) for a given c-C_3H_6 pressure were obtained by plotting ln (Rate) vs $1/T$ (K) using the relationship

$$\text{Rate} = kf(**, pC_3H_6), \qquad (4)$$

and the Arrhenius Equation,

$$\ln k = \ln(A) - (E_a/R)(1/T), \qquad (5)$$

where A is the pre-exponential factor and E_a is the apparent activation energy.

C. Transient Kinetics

Transient kinetics studies were done with a stainless steel microreactor having responses that behave as an ideal mixed-flow reactor with Nuclide 12-90-G mass spectrometer and gas chromatograph detectors. Both transient isothermal sorption uptake and temperature programmed desorption (TPD) experiments were carried out with a gas mixture of 0.5% c-C_3H_6 in Ar and Ar as a carrier gas, respectively. Step changes of the feed and in TPD experiments have been described (*11*). Further details concerning operation of this system and experimental procedures can be found elsewhere (*11–14*).

D. Fourier Transform Infrared Spectroscopy

Fourier transform infrared (FTIR) spectroscopy experiments were performed on a Mattson Galaxy spectrometer with a homebuilt *in situ* IR cell. After dehydration of the EuNaX zeolite samples in this cell, pyridine gas was used to sorb on Lewis and Brønsted sites of the zeolites. Pellets of 15-mg EuNaX zeolite (neat) or mixed with silicalite were used in these studies with samples dehydrated at 380°C under vacuum at 2×10^{-5} Torr for 8 h. Adsorption of pyridine was done at room temperature for 2 h. Physisorbed pyridine was then desorbed at 1×10^{-5} Torr at 150°C overnight. Pellets doped with silicalite as an internal standard were also investigated. Peaks at 1541 cm^{-1} were integrated to determine the relative number of Brønsted acid sites in the various loadings of Eu^{3+} in NaX zeolites. These peaks were compared to Lewis peaks at 1460 cm^{-1} as well as an internal standard of silicalite.

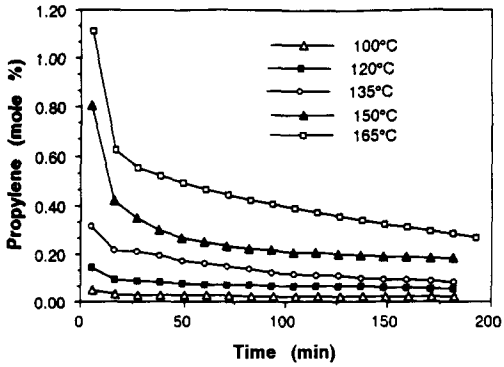

FIG. 2. Gas composition of propylene vs time-on-stream, 0.10 M Eu^{3+}NaX.

E. Atomic Absorption

Bulk analyses were done with a Techtron atomic absorption spectrometer by using a Li fusion method for sample dissolution and standard addition methods to determine the Eu^{3+} concentrations in the three different loaded zeolite samples.

III. RESULTS

A. Steady-State Kinetics

Catalytic data for the highest Eu^{3+} loading (0.10 M exchange solution) in NaX are shown in Fig. 2. The mol% propylene product decreases in time out to about 150 min for reaction temperatures of 100, 120, 135, 150, and 165°C. The higher the reaction temperature, the greater the amount of propylene product. These data were collected for a 9.09% c-C_3H_6/He feed at 1 atm total pressure. Note that after each run at a specific temperature (experiments done from low T to High T) that the samples were treated in He at 380°C. GC analyses of gases desorbed

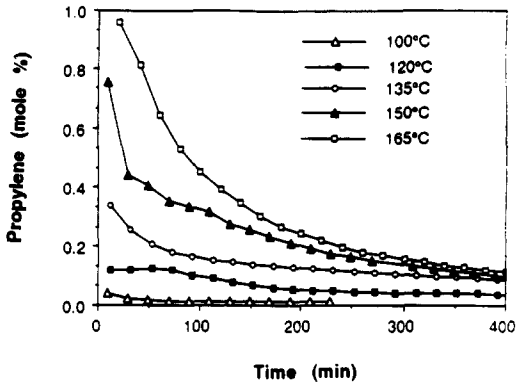

FIG. 3. Gas composition of propylene vs time-on-stream, 0.05 M Eu^{3+}NaX.

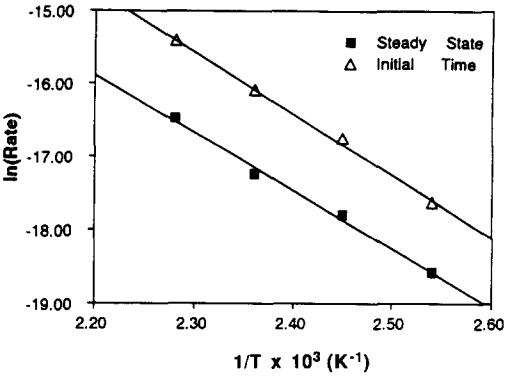

FIG. 5. Arrhenius plot of ln (Rate) vs $1/T$ for initial and steady-state times, 0.01 M Eu^{3+}NaX.

during these regeneration processes were consistent with the desorption of C_3H_6.

Catalytic data for the intermediate Eu^{3+} loading (0.05 M) in NaX of Fig. 3 show similar trends, although steady state is reached at longer times, approximately 350–400 min. In addition, the yields of C_3H_6 are somewhat diminished with respect to the highest Eu^{3+} loaded NaX sample, for example, from 0.8 mol% propylene at 150°C for the highest Eu^{3+} loading to 0.75 mol% propylene at 150°C for the intermediate Eu^{3+} loading catalyst.

The activation energies for propylene formation are 15.9 and 13.2 kcal/mol for initial times and steady state times, respectively for the highest Eu^{3+} loading material as shown in Fig. 4. The activation energies for the lowest Eu^{3+} loading (0.01 M) catalyst are 16.8 and 15.7 kcal/mol for initial and steady state times, respectively, as shown in Fig. 5.

The rates of propylene formation at 135°C and for various partial pressures of c-C_3H_6 in the feed are shown in Fig. 6. Rates of C_3H_6 formation increase as the partial pressure of c-C_3H_6 are increased from 3.8 Torr to 30, 69, and 197 Torr.

A plot of ln (Rate) vs ln P(c-C_3H_6) for the lowest Eu^{3+} loading of NaX is shown in Fig.

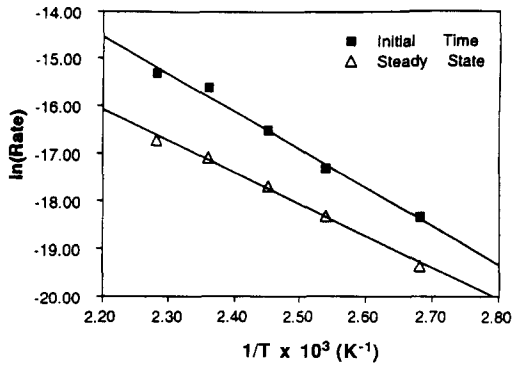

FIG. 4. Arrhenius plot of ln(Rate) vs $1/T$ for initial and steady-state times, 0.10 M Eu^{3+}NaX.

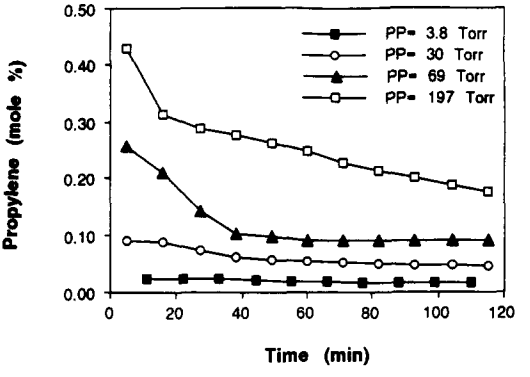

FIG. 6. Gas Composition of propylene vs time-on-stream, 0.01 M Eu^{3+}NaX at various partial pressures of cyclopropane.

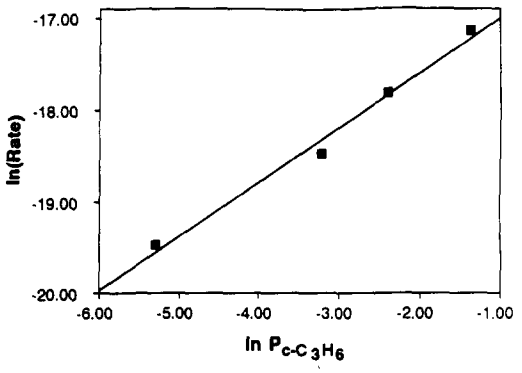

FIG. 7. Plot of ln (Rate) vs ln (Partial Pressure of c-C_3H_6), 0.10 *M* Eu^{3+}NaX, T = 135°C.

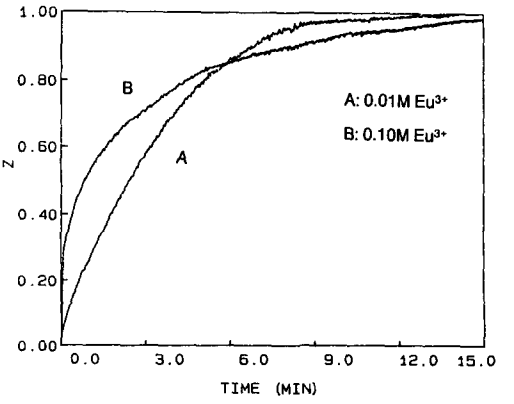

FIG. 9. Transient sorption plot of dimensionless response (*Z*) vs time-on-stream for (A) 0.01 *M* Eu^{3+}NaX, (B) 0.10 *M* Eu^{3+}NaX. Sequence is Ar purge → sorption of 0.5% c-C_3H_6 in Ar at 30 cc/min flow rate at 40°C.

7. Data from the slope of this plot can be used to determine the reaction order of c-C_3H_6 which is approximately 3/5 order.

Plots of the activation energies for propylene formation as a function of Eu^{3+} loading for both initial and steady state times are given in Fig. 8. These data show that as the Eu^{3+} loading increases from 0.01 *M* for the lowest loading to 0.10 *M* for the highest loading that the activation energy steadily decreases for both initial (5 min) and steady-state (180 min) times.

Eu^{3+} NaX after calcination was also reacted with Na vapor on a vacuum line at 1×10^{-5} Torr at temperatures above 200°C. The samples exposed to Na vapor were not active in cyclopropane ring opening until at least 325°C where slight activity was noticed.

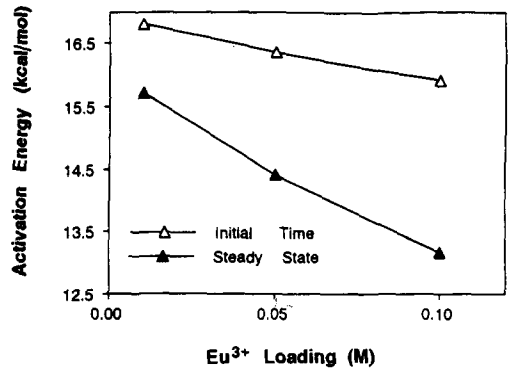

FIG. 8. Activation energies vs Eu^{3+} loading, corresponding to initial and steady-state times.

B. Transient Kinetics

(*1*) *Sorption data.* Transient sorption kinetics for a 0.5% c-C_3H_6 in Ar mixture at 40°C for the lowest Eu^{3+} and highest Eu^{3+} loadings are shown in Fig. 9, A and B, respectively. The *y* axis is the dimensionless gas phase concentration (*Z*) of c-C_3H_6 measured by mass spectrometry. It is the ratio of gas phase c-C_3H_6 measured at some time *t* to the gas phase c-C_3H_6 concentration at infinite time. *Z*, therefore, has limits of 0 and 1, the latter being at saturation (equilibrium). The gas phase concentration of c-C_3H_6 for the lowest Eu^{3+} loading (Fig. 9(A)) at times less than about 5 min is less than that for the corresponding highest Eu^{3+} loading (Fig. 9(B)).

The gas phase concentration of c-C_3H_6 for the lowest Eu^{3+} loading catalyst reaches equilibrium around 14 min, whereas the highest Eu^{3+} loading catalyst does not quite reach steady state even after 15 min. These observations will be explained in the discussion section.

Sorption data for a mixture of 0.5% C_3H_6 in Ar in the lowest and highest Eu^{3+} loading

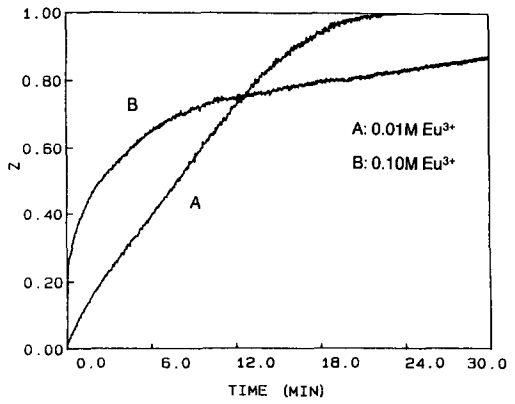

FIG. 10. Transient sorption plot of dimensionless response (Z) vs time-on-stream for (A) 0.01 M Eu^{3+} NaX, (B) 0.10 M Eu^{3+}NaX. Sequence is Ar purge → sorption of 0.5% C_3H_6 in Ar at 30 cc/min flow rate at 40°C.

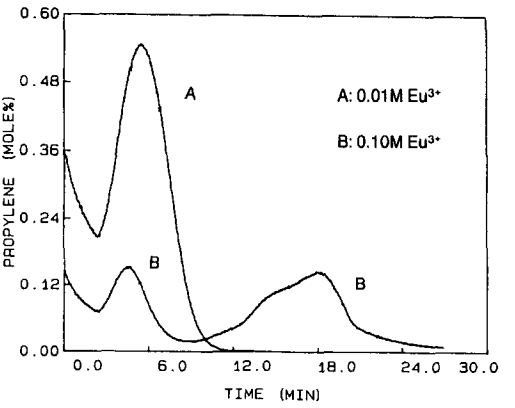

FIG. 12. Temperature programmed desorption of c-C_3H_6 for (A) 0.01 M Eu^{3+}NaX, (B) 0.10 M Eu^{3+} NaX. Sequence is sorption of 0.5% c-C_3H_6 in A rat 30 cc/min flow rate at 40°C, 30 min → Ar Purge (120 sec) → TPD (β = 15°C/min).

catalysts are shown in Fig. 10, A and B, respectively. The shapes of these gas phase sorption curves are somewhat different from those for c-C_3H_6 as shown in Fig. 9; however, the faster uptake (slower gas phase response) of C_3H_6 for the lowest Eu^{3+} loading with respect to the highest Eu^{3+} loading catalyst is again evident. For the highest Eu^{3+} loading material, the Z value takes more than 30 min to reach 1.

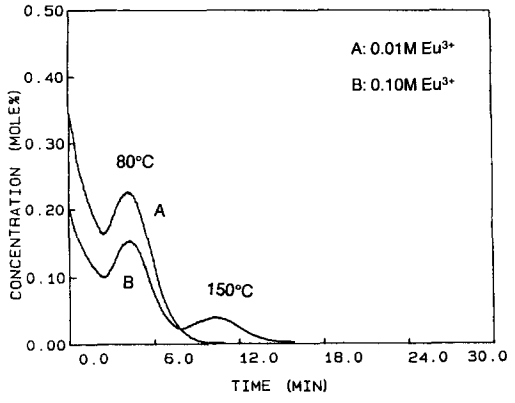

FIG. 11. Temperature programmed desorption of c-C_3H_6 for (A) 0.01 M Eu^{3+}NaX, (B) 0.10 M Eu^{3+} NaX. Sequence is sorption of 0.5% c-C_3H_6 in A rat 30 cc/min flow rate at 40°C, 15 min → Ar Purge (120 sec) → TPD (β = 15°C/min).

(2) *Desorption data.* Temperature programmed desorption data for the lowest and highest Eu^{3+} loadings in NaX for a mixture of 0.5% c-C_3H_6 in Ar are shown in Fig. 11, A and B, respectively. These experiments were performed by first sorbing c-C_3H_6, followed by a purge of the gas stream with Ar for 120 sec and then a temperature programmed desorption in Ar at 15°C/ min. These TPD data show that the lowest Eu^{3+} loading in NaX catalyst has one major desorption peak with a maximum temperature (T_M) of 80°C. The highest Eu^{3+} loading catalyst has two T_M's, one at 80°C, the other at 150°C. The relative amount of c-C_3H_6 for the first T_M peak at 80°C for the lowest Eu^{3+} loading NaX sample is 0.48 mmol/g whereas the amount for the highest loading Eu^{3+} NaX catalyst is 0.36 mmol c-C_3H_6/g catalyst.

The effluent was analyzed for c-C_3H_6, C_3H_6 and oligomerized species such as hexenes via mass spectrometry as well as gas chromatography (GC) for the different peaks of Figs. 11 and 12. GC results show that C_3H_6 was detected for only the desorption peak at higher temperatures.

Similar TPD data for C_3H_6 from the lowest and highest Eu^{3+} loading materials after

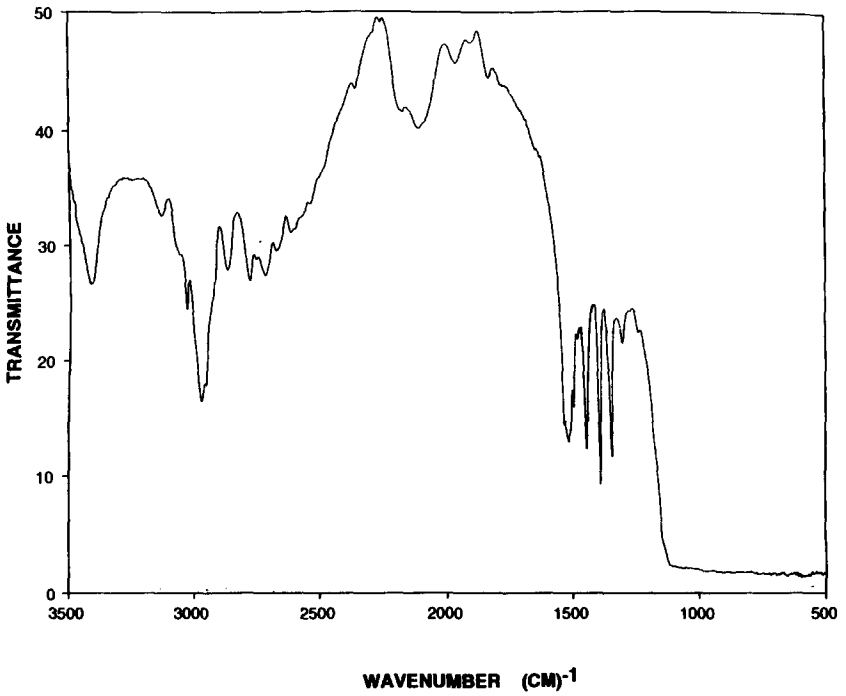

FIG. 13. Fourier transform infrared spectrum of pyridine chemisorbed on 0.10 *M* Eu^{3+}NaX. Dehydration of zeolite at 380°C, followed by room-temperature sorption of pyridine, and then removal of physisorbed pyridine overnight at 150°C and 1×10^{-5} Torr.

sorption of 0.5% C_3H_6 in Ar at 40°C are shown in Fig. 12, A and B, respectively. The amount of C_3H_6 under the T_M peak at 90°C for the lowest Eu^{3+} loading catalyst is 1.1 mmol C_3H_6/g catalyst. The total amount of C_3H_6 under the whole curve for the highest Eu^{3+} loading NaX catalyst represented by three peaks with T_M values of 80, 225, and 290°C is 0.66 mmol C_3H_6/g catalyst.

C. FTIR Data

An FTIR spectrum of the highest Eu^{3+} loading in NaX zeolite after dehydration at 380°C, followed by room-temperature sorption of pyridine and evacuation of physisorbed pyridine overnight at 150°C is shown in Fig. 13. A sharp band at 1541 cm^{-1}, a band at 1460 cm^{-1}, and a band at 2,000 cm^{-1} are observed. Similar bands are observed for all three Eu^{3+} loadings. The ratio of the intensity of the 1541-cm^{-1} band to the 2,000-cm^{-1} band for the lowest Eu^{3+} loading NaX zeolite is 1.08, whereas the same ratio for the highest Eu^{3+} loading material is 1.42. The ratios of intensities of the 1541-cm^{-1} peak to the 1460-cm^{-1} peak for the 0.01 *M* Eu^{3+}NaX material is 6.02, whereas the same ratio for the 0.10 *M* Eu^{3+} NaX zeolite sample is 5.55. All ratios were obtained by integrating absorbance data.

D. Bulk Analyses

The lowest loading (0.01 *M*) Eu^{3+} sample was found to have 14.95 Eu^{3+} ions/unit cell, the 0.05 *M* Eu^{3+} intermediate loading NaX zeolite was found to have 19.76 Eu^{3+} ions/unit cell, and the 0.10 *M* Eu^{3+} loading NaX material was found to have 20.49 Eu^{3+} ions/unit cell as determined by atomic absorption analyses.

Note that the number of ions per unit cell as a function of increased loading does not increase linearly. The amount of Eu^{3+} incorporated during exchange does increase,

however, as the molarity of the exchange solution reaches 0.10 *M*. The rate of increase of Eu^{3+} incorporation with respect to solutions of lowest molarity is diminished. This is usually the case for ion-exchange at high levels of exchange due to the decreased availability of exchangeable sites.

IV. DISCUSSION

A. Steady-State Results

The data of Figs. 2 and 3 for the highest and intermediate Eu^{3+} loading materials show an appreciable decrease in activity with time on stream. The rate of deactivation of the Eu^{3+} catalysts is greater for the highest Eu^{3+} loading than for the lower loadings. This is probably so because the higher Eu^{3+} loading catalysts have a distribution of stronger acid sites that are likely to be poisoned by the c-C_3H_6 reactant and C_3H_6 product due to their ability to sorb these molecules more strongly than lower loading materials.

The activation energy for ring opening of gas phase cyclopropane is 54 kcal/mol (*25*), significantly greater than values reported here. A 1,3 biradical intermediate species has been proposed on the basis of deuterium labeling (*25*). This may suggest that such intermediates are not present in our systems.

The data of Figs. 6 and 7 clearly show that the partial pressure of c-C_3H_6 affects the yield of C_3H_6 and the rate of reaction. The 3/5 reaction order indicates that dissociation of c-C_3H_6 is an important step in the overall mechanism which will be discussed later. The lowest Eu^{3+} loading samples were only used to determine reaction order to minimize effects caused by deactivation and site poisoning.

Poisoning of H^+ sites by Na vapor led to deactivation of the catalysts according to

$$Na(g) + H^+ \rightleftharpoons \frac{1}{2} H_2\uparrow + Na^+ \qquad (9)$$

the equilibrium of Eq. 9. These data strongly suggest that at least on these Eu^{3+} catalysts that Brønsted sites are primarily responsible for ring opening of cyclopropane.

B. Transient Kinetics

Transient kinetic data for sorption of c-C_3H_6 of Fig. 9 show that the lowest Eu^{3+} loading material initially has a greater uptake of c-C_3H_6 than the highest Eu^{3+} loading material. The fact that the highest Eu^{3+} loading material shows a transient response that does not reach equilibrium even after 15 min indicates that either some of the c-C_3H_6 is reacting or that there are significant holdup times from diffusional restrictions in the zeolite.

The fact that similar trends are observed for sorption of C_3H_6 (Fig. 10) and that there was no observation of reaction of cyclopropane at temperatures near 40°C suggest that there must be diffusional restrictions for both c-C_3H_6 and C_3H_6 in the transient sorption experiments of Figs. 9 and 10. Such diffusional limitations may markedly affect rates measured in our experiments. Mass spectrometry data show small amounts (<1%) of C_6 hydrocarbons which are desorbed from these catalysts during TPD experiments. No isobutane was observed in contrast to studies of c-C_3H_6 over other zeolites (*5*, *6*).

The use of He at 380°C to regenerate the catalyst appears to be fruitful based on results of rate measurements before and after regeneration. These observations and TPD experiments suggest that oligomerized species like hexenes are desorbed during this process.

The TPD data of Fig. 11 show that for the lowest Eu^{3+} loading catalyst that primarily one peak is observed having a T_M of about 80°C. Gas chromatography experiments confirm that this peak is due to sorbed c-C_3H_6. The second peak, only observed with the highest Eu^{3+} loading material at 150°C, is due to desorption of C_3H_6 product formed on reaction with c-C_3H_6 as evidenced by GC analysis.

TPD data for desorption from samples exposed to C_3H_6 as shown in Fig. 12 show

$$Eu(H_2O)_x^{n+} \longrightarrow Eu(OH)_x^{(n-x)+} + H^+$$

$$4\,Eu(H_2O)_9^{3+} \longrightarrow Eu_4O^{10+} + 35\,H_2O + 2H^+$$

SCHEME I. Generation on Brønsted sites in Eu^{3+}NaX.

several peaks at temperatures greater than 100°C which are due to desorption of C_3H_6 from several sites, at least on the highest Eu^{3+} loading NaX catalyst. While such peaks were not observed for the lowest Eu^{3+} loading catalysts this does not preclude small populations of such sites in these materials which might be expected to have broad TPDs. In any event it is clear that the highest Eu^{3+} loading catalysts have a variety of available sites with variable acid strengths.

C. Mechanistic Ideas

A general scheme for the generation of Brønsted sites in rare earth zeolites such as Eu^{3+}NaX is shown in Scheme I. On dehydration, Brønsted sites are generated and Eu^{3+} ions are believed to migrate into sodalite cages (*7–10*) of the zeolite to form a tetrahedral $[Eu_4O]^{10+}$ complex as shown in Fig. 14, which has been identified by single crystal X-ray powder diffraction experiments (*7*). The $Eu(H_2O)_9^{3+}$ species is proposed to exist in the supercage of EuNaX zeolite on the basis of EXAFS and luminescence lifetime experiments (*8*).

Data from FTIR experiments of Fig. 13 conclusively show that Brønsted sites are generated in these Eu^{3+} zeolites and similar data for the three different Eu^{3+} loadings show that as the Eu^{3+} loading increases that the relative number of Brønsted sites (with respect to the silicalite internal standard) also increases. The relative number of Lewis sites with respect to the 2,000 cm^{-1} band for silicalite increased, while the relative intensity of the Brønsted to Lewis peaks at 1541 to 1460 cm^{-1} decreased as reported in the results section. All other peaks observed in FTIR spectra are consistent with framework Si–O and Al–O vibrations.

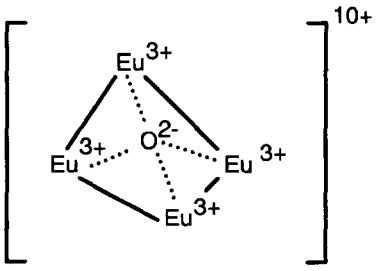

FIG. 14. Tetrahedral $[Eu_4O]^{10+}$ complex found on Sodalite cages of Eu^{3+}NaX.

This does not imply that Lewis sites (which also increase at higher loading) may not also be active in transformations of c-C_3H_6 in these systems. However, the increased conversion, increased number of peaks in the TPD data at high temperature, and FTIR data suggest a correlation between Brønsted sites and catalytic activity.

The Na vapor experiments also suggest that Brønsted sites are poisoned with concomitant loss in activity. NaX itself is not active in ring opening until temperatures of 300°C or higher. We do not expect Na vapor to poison either Na^+ or Eu^{3+} Lewis sites, whereas reaction of Na with H^+ is well known (*26, 27*).

A reaction mechanism to explain these observations is shown in Scheme II for transformation of c-C_3H_6 to a Brønsted acid bound cyclopropane which may rearrange to a pi bound intermediate with subsequent release of C_3H_6.

TPD and FTIR data suggest that higher loadings of Eu^{3+} generate stronger and more Brønsted acid sites than lower Eu^{3+} catalysts. Although poisoning of the strongest sites occurs first as evidenced by the increased rate of deactivation as the Eu^{3+} loading is increased, presumably not all of the strong sites become inactive within the timescale of the experiment and these sites contribute to product conversion at steady state. All active sites are in the supercages of EuNaX because the kinetic diameter of c-C_3H_6 is 4.2 Å, thereby preventing diffu-

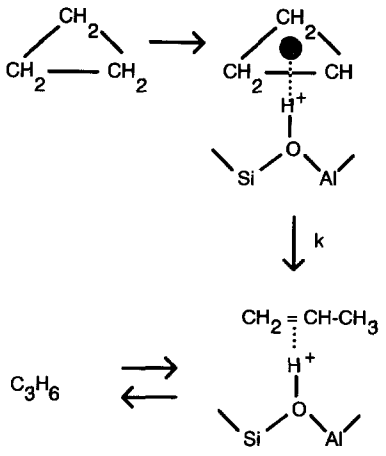

SCHEME II. Proposed reaction mechanism for cyclopropane isomerization on EuNaX.

sion of c-C_3H_6 into sodalite cages which have an opening of 2.2 Å. Further evidence that Eu^{3+} sites are inaccessible in sodalite cages comes from recent NMR studies of lanthanide faujasite systems (*28*).

Catalysts were regenerated in He after every run before catalysis reactions were done at higher temperatures in order to get rid of coke deposits which were indicated by the steady-state and transient data of Figs. 2, 3, 6, and 9–12. The coke is primarily due to bound propylene perhaps bound through an allyl intermediate. The π character of the C_3H_6 makes it a strong sorbent as evidenced by the transient TPD data. Traces of hexenes (<5 ppm) have also been observed in mass spectrometry experiments and may be partially responsible for coke deposits.

The mechanism of bonding of c-C_3H_6 proposed in Scheme II is similar to that proposed by Brady and Gorte (*4*), however, in their studies with H-ZSM5 no propylene was observed during desorption experiments. These data suggest that the relative acidities of the Eu^{3+}NaX and H-ZSM5 systems may be markedly different. Since propylene is readily desorbed from Eu^{3+}NaX, catalytic intermediates may be bound propylene-like species that tend to block active ring opening sites.

The transient desorption data of Figs. 11 and 12 show that the total uptake of propylene (1.76 mmol/g catalyst) is significantly greater than for cyclopropane uptake (0.84 mmol/g catalyst). These data suggest that the cyclopropane moiety having larger size and with π electron density spread between 3 carbon atoms has greater steric and electronic repulsion that propylene which can sorb to more cation and inner wall sites. Transient sorption data of Figs. 9 and 10 are also in accord with this assertion.

Further support for the mechanism described in Scheme II comes from various spectroscopic experiments such as infrared (*2, 15, 16*), NMR (*17*), electron spectroscopy (*18*), and ultraviolet visible spectroscopy (*2*), where π allyl intermediates have been proposed primarily for Brønsted acid sites in mordenite, faujasites and other zeolites. Few researchers have suggested that Lewis sites are the active sites in the isomerization of c-C_3H_6, except for work with Co^{2+}A zeolite (*19*). The transient desorption data of Figs. 11 and 12 suggest that the 2nd TPD peak of Fig. 11 is due to Brønsted sites. The transient data of Fig. 12 suggest that propylene is most tightly bound to different sites than the Brønsted site observed in Fig. 11.

Activation energies for formation of propylene from c-C_3H_6 in organometallic catalysis (*20*) such as in the formation of carbenes are on the order of 17 kcal/mol. Heterogeneous catalysts of Ni on SiO_2 (*21*) and Ru NaX zeolites (*22*) have also been used to isomerze c-$C_{3+}H_6$ and activation energies on the order of 14–17 kcal/mol have been observed. Metal-containing zeolites often lead to hydrogenolysis such as with Pd and Pt Y zeolites (*23*). No hydrogenolysis was observed with Eu^{3+}NaX, however, Ni^{2+} NaX does show hydrogenolysis of c-C_3H_6 to methane and ethane (*24*).

V. CONCLUSIONS

Steady state, transient kinetic and FTIR data have shown that Eu^{3+}NaX zeolite catalysts can be used to selectively isomerize

cyclopropane to propylene with rapid deactivation being due to the formation of an intermediate, which is primarily bound propylene. Minor amounts of coke in the form of hexenes are detected at the 5-ppm level from TPD experiments. Increased loading of Eu^{3+} gives rise to lower activation energies for the isomerization of cyclopropane and higher propylene sorption and cyclopropane isomerization reaction rates. FTIR and catalytic studies suggest that increased loadings of Eu^{3+} produce more Brønsted acid sites with respect to types and amounts in NaX than lower Eu^{3+} loaded materials. TPD and deactivation studies show that higher Eu^{3+} loadings produce stronger acid sites than lower Eu^{3+} loading materials. Apparent activation energies are initially higher than at steady state conditions and values of 13–15 kcal/mol are consistent with literature values for isomerization of cyclopropane over other supported metal catalysts.

ACKNOWLEDGMENTS

We acknowledge the support of the Department of Energy, Office of Basic Energy Sciences, Division of Chemical Sciences for this research and Don Hobro for assistance with AA.

REFERENCES

1. (a) Efstathiou, A. M., Suib, S. L., and Bennett, C. O., *J. Catal.*, in press; (b) **131,** 94 (1991).
2. Kirisci, I., and Förster, H., *J. Chem. Soc. Far. Trans. 1* **84**(2), 491 (1988).
3. Jacobs, P. A., "Carbogenionic Activity of Zeolites." Elsevier, Amsterdam, 1977.
4. Grady, M. C., and Gorte, R. J., *J. Phys. Chem.* **89,** 1305 (1985).
5. (a) Fejes, P., Kirisci, I., Tasi, G., and Varga, K., *in* "Proceedings, International Conference on Zeolite Catalysis, Siofok, 1985," p. 405; (b) Förster, H., Franke, S., Seebode, J., *J. Chem. Soc. Faraday Trans. 1* **79,** 373 (1983).
6. Förster, H., and Seebode, J., *in* Proceedings, International Conference on Zeolite Catalysis, Siofok, 1985," p. 413.
7. Olson, D. H., Kokotailo, G. T., and Charnell, J. F., *J. Colloid Interface Sci.* **28,** 305 (1968).
8. Suib, S. L., Zerger, R. P., Stucky, G. D., Morrison, T. I., and Shenoy, G. K. *J. Chem. Phys.* **80,** 2203 (1984).
9. Suib, S. L., Zerger, R. P., Stucky, G. D., Emberson, R. M., Debrunner, P. G., and Iton, L. E. *Inorg. Chem.* **19,** 1858 (1980).
10. Iton, L. E., Suib, S. L., and Stucky, G. D., *Bull. Magn. Res.* **2,** 4086 (1981).
11. Efstathiou, A. M., and Bennett, C. O., *J. Catal.* **120,** 137 (1989).
12. Stockwell, D. M., Chung, J. S., and Bennett, C. O., *J. Catal.* **112,** 135 (1988).
13. Efstathiou, A. M., and Bennett, C. O., *J. Catal.* **120,** 118 (1989).
14. Stockwell, D. M., and Bennett, C. O., *J. Catal.* **110,** 354 (1988).
15. Bartlett, J. R., Cooney, R. P., and Kydd, R. A., *J. Catal.* **114,** 53 (1988).
16. Kiricsi, I., Tasi, G., Fejes, P., and Berger, F. *J. Mol. Catal.* **51,** 341 (1989).
17. Susic, M. V., Vucelic, D. R., Karaulic, D. B., and Pausak, S. V. *Surf. Sci.* **18,** 204 (1969).
18. Klier, K., *Adv. Chem. Ser.* **101,** 480 (1971).
19. Corma, A., and Wojciechowski, B. W., *Catal. Rev. Sci. Eng.* **27,** 29 (1985).
20. Collman, J. P., and Hegedus, L. S. "Principles and Applications of Organotransition Metal Chemistry." pp. 508–520. University Science Press, Mill Valley, CA, 1980.
21. Coenen, J. W. E., Schats, W. M. T. M., and van Meerten, R. Z. C., *Bull. Soc. Chim. Belg.* **88,** 435 (1979).
22. Schwank, J., Lee, J. Y., and Goodwin, J. G., *J. Catal.* **108,** 495 (1987).
23. Bai, X., and Sachtler, W. M. H. *J. Catal.* **132,** 266 (1991).
24. Simon, M. W., Efstathiou, A. M., Bennett, C. O., and Suib, S. L., in preparation.
25. Benson, S., "Thermochemical Kinetics," pp. 117–128. Wiley, New York, 1976.
26. Jacobs, P. A., Jaeger, N. I., Jiru, P., and Schultz-Ekloff, G., "Metal Microstructures in Zeolites," Studies in Surface Science Series, Vol. 12. Elsevier, New York, 1982.
27. Lee, J. B., *J. Catal.* **68,** 27–32 (1981).
28. Chao, K. J., Chen, S. H., Liu, S. H., Inui, T., Namba, S., and Tatsumi, T., *Stud. Surf. Sci. Catal.* **60,** 123–131 (1991).